

Ab initio study in the island of inversion within the two-major-shell valence space

X. C. Cao^{a,b}, C. F. Jiao^{a,b,*}

^a*School of Physics and Astronomy, Sun Yat-sen University, Zhuhai, 519082, Guangdong, China*

^b*Guangdong Provincial Key Laboratory of Quantum Metrology and Sensing, Sun Yat-sen University, Zhuhai, 519082, Guangdong, China*

Abstract

We present an *ab initio* study of nuclear structure in the island of inversion around neutron number $N = 20$, using multishell effective Hamiltonians derived from valence-space in-medium similarity renormalization group approach combined with the quantum-number projected generator coordinate method. By progressively expanding the valence space from the sd shell to the intermediate $sd f_{7/2} p_{3/2}$ space and, for the first time, to the full $sd fp$ shell, we investigate low-lying spectra, $E2$ transition strengths, deformation properties, and neutron occupancies in even-even Ne, Mg, and Si isotopes around $N = 20$. Our results show that enlarging the valence space significantly improves the description of quadrupole collectivity, yielding better agreement with experimental data for key observables such as the lowered 2^+ energies and the enhanced $B(E2; 0_1^+ \rightarrow 2_1^+)$ values. The analysis reveals the critical role of cross-shell multi-particle multi-hole excitations in breaking the $N = 20$ shell closure and establishing intruder-dominated ground states. It also demonstrates the ability of the VS-IMSRG+PGCM framework to capture both dynamical (short range) and static (long range) correlations across multiple major-oscillator shells.

Keywords: Nuclear *ab initio* method, Valence-space in-medium similarity renormalization group, Projected generator-coordinate method, Island of inversion

1. Introduction

Shell structure is a common characteristic of a finite quantum many-body system. In atomic nuclei, the shell structure and the associated “magic numbers”, governed by inter-nucleon interactions, has been extensively studied since the pioneering work of Mayer and Jensen [1, 2]. The advent of large-scale rare-isotope beam facilities has opened up opportunities to explore novel shell structures in unstable exotic nuclei. A particularly intriguing discovery is the so-called *island of inversion* [3, 4, 5, 6, 7], where conventional shell closures break down and the nuclei exhibit unexpectedly enhanced quadrupole collectivity [8, 9, 3]. This phenomenon was first identified through the disappearance of the neutron magic number $N = 20$ in neutron-rich neon, sodium, and magnesium isotopes [10, 9, 11], challenging the traditional understanding of magic numbers and sparking considerable interest in elucidating the mechanisms underlying shell evolution [12, 13, 14].

Substantial efforts, both experimental [11, 15, 16, 10, 17, 18, 19, 20, 21] and theoretical [22, 14, 23, 13, 24, 4], have been devoted to understanding the island of inversion. These studies have established that the ground-state (g.s.) wave functions of nuclei in this region are dominated by intruder configurations, primarily involving multi-particle multi-hole (*mp-mh*) excitations from the sd to the fp orbits [3, 25, 8]. This is attributed to a weakening of the $N = 20$ shell gap between the two major oscillator shells, leading to the disappearance of the traditional

magic number. Although certain phenomenological approaches have succeeded in reproducing the enhanced quadrupole collectivity, these studies typically rely on nuclear interactions that are empirically fine-tuned to existing data on finite nuclei. This dependence limits their predictive power for exotic nuclei far from the valley of stability, where experimental data are scarce.

During the past two decades, significant progress has been made in developing *ab initio* nuclear structure methods [26, 27, 28, 29, 30, 31, 32, 33]. These approaches aim to describe nuclear properties directly from the fundamental inter-nucleon interactions [e.g., nucleon–nucleon (NN) and three-nucleon ($3N$) interactions derived from chiral effective field theory (χ EFT)] and retain the connection to quantum chromodynamics (QCD) [34, 35, 36], without relying on empirical adjustments beyond those necessary to constrain the nuclear forces themselves. Despite promising advances in *ab initio* methods, microscopic understanding of the island of inversion from the fundamental nuclear forces still poses a challenge. Recently, the extended Kuo-Krenciglowa (EKK) method based on many-body perturbation theory (MBPT) has been used to perturbatively derive an effective Hamiltonian within the $sd fp$ shell from the chiral nuclear force [4], but it still empirically fits the single-particle energies to accurately describe the island of inversion.

The valence-space in-medium similarity renormalization group (VS-IMSRG) is a powerful non-perturbative *ab initio* framework capable of computing a wide range of nuclear observables—including energies, charge radii, and electroweak moments and transitions—for both ground and excited states in open-shell nuclei [37, 38, 39, 40, 41, 8]. It starts from chiral NN and $3N$ interactions and non-perturbatively decou-

*Corresponding author.

Email address: jiaochf@mail.sysu.edu.cn (C. F. Jiao)

ples an effective Hamiltonian within a chosen valence space. The diagonalization of this Hamiltonian, typically via the shell model, then yields the eigenvalues and wave functions of the many-body system. However, a major difficulty in applying the VS-IMSRG to the island of inversion is the need to incorporate intruder configurations that involve multiple major shells (the *sd* and *fp* shells). In conflict with it, deriving effective Hamiltonians has generally been restricted to single major-shell valence spaces due to the computational limitations of conventional shell model diagonalization. Recently, the VS-IMSRG derived the first *ab initio* multishell valence-space Hamiltonians for this region [8, 42], but the valence space is limited to the $\pi sd + \nu sd f_{7/2} p_{3/2}$ shell. It does not reproduce the lowered 2_1^+ state and strong electric quadrupole transitions for ^{32}Mg , indicating that the effective Hamiltonians within the $\pi sd + \nu sd f_{7/2} p_{3/2}$ shell may not fully capture the enhanced quadrupole collectivity. A complete treatment of cross-shell *mp-mh* excitations from the *sd* to the *fp* shells requires effective Hamiltonians spanning the full two major oscillator shells (*sdfp*).

Diagonalizing *sdfp*-shell Hamiltonians is computationally prohibitive within the conventional shell model. Alternatively, the quantum-number projected generator coordinate method (PGCM) has been established as an outstanding variational approximation to exact diagonalizations in shell-model valence spaces [43, 44, 45, 46, 47, 48]. In addition, the PGCM can be readily extended to very large model spaces [43]. Given the demonstrated success of the valence-space extension within the VS-IMSRG framework in improving the descriptions of cross-shell correlations and enhanced quadrupole collectivity [8, 42], the PGCM presents a natural choice over the conventional shell model.

In this work, we exploit the VS-IMSRG approach to decouple the *ab initio* valence-space Hamiltonians spanning the *sd*, the *sd f_{7/2} p_{3/2}*, and the *sd fp* shell. These effective Hamiltonians are then used in the PGCM calculations to systematically study the island of inversion with progressively expanded valence spaces. We demonstrate the improvement achieved by the expansion of the valence spaces in describing the low-lying spectroscopic properties of island-of-inversion nuclei using the VS-IMSRG effective Hamiltonians. We also provide a detailed analysis of the *mp-mh* excitations from the *sd* to the *fp* shell across two full major oscillator shells. Other novel *ab initio* frameworks, such as the angular-momentum projected coupled cluster theory with singles and doubles (AMP-CCSD) [49, 50, 51] and the in-medium generator-coordinate method (IM-GCM) [45, 52] that combines the PGCM and multi-reference IMSRG (MR-IMSRG) [53, 54], have also been applied to this region. While achieving remarkable success in describing strongly deformed rotational bands [49, 50, 51] and shape co-existence [25], their applications to heavier nuclei are severely constrained by high computational costs. Alternatively, the valence-space-based VS-IMSRG+PGCM framework employed here offers a scalable path for future *ab initio* studies of heavier open-shell nuclei.

2. The model

In the valence-space framework, the single-particle Hilbert space is partitioned into core, valence, and outside subspaces. The core orbitals (i.e., ^{16}O in this work) and outside orbitals are treated as inactive in the final calculations. In the valence space, the effective Hamiltonian, which encodes the essential degrees of freedom for reproducing low-lying states, is constructed to account for possible configuration mixing through exact diagonalization or PGCM approach here. Therefore, our objective is to develop an effective Hamiltonian where excitations out of the core or into the outside subspaces are rigorously decoupled. To achieve this decoupling, the IMSRG evolves the initial Hamiltonian via a continuous unitary transformation governed by the flow equation given by

$$\frac{dH(s)}{ds} = [\eta(s), H(s)], \quad (1)$$

where the Hamiltonian, which depends on the flow parameter s , is expressed in the second-quantized form:

$$H(s) = E_0 + \sum_{ab} f_{ab}(s) \{a_a^\dagger a_b\} + \frac{1}{4} \sum_{abcd} \Gamma_{abcd}(s) \{a_a^\dagger a_b^\dagger a_d a_c\}. \quad (2)$$

E_0 , f_{ab} , and Γ_{abcd} denote the zero-, one-, and two-body matrix elements of the Hamiltonian, respectively. a_a (a_a^\dagger) is the operator that annihilates (creates) a particle in the single-particle orbital labeled by a . The $\{\dots\}$ indicates normal ordering with respect to the reference state, which can be a single Slater determinant or an ensemble state [37]. The anti-Hermitian operator $\eta(s)$ is the so-called generator written as

$$\eta = \sum_{ai} \eta_{ai} \{a_a^\dagger a_i\} + \sum_{abij} \eta_{abij} \{a_a^\dagger a_b^\dagger a_j a_i\} - \text{H.c.} \quad (3)$$

with

$$ai \in \{pc, ov\}, \quad abij \in \{pp'cc', pp'vc, opvv'\}. \quad (4)$$

The indices c , v , and o indicate core, valence, and outside space orbitals, respectively, and p denotes either v or o . For we need to derive effective Hamiltonians spanning multiple major oscillator shells, the generator is defined as

$$\eta_{ai} = \frac{1}{2} \arctan \left(\frac{2f_{ai}}{f_{aa} - f_{ii} + \Gamma_{aiai} + \Delta} \right), \quad (5)$$

$$\eta_{abij} = \frac{1}{2} \arctan \left(\frac{2\Gamma_{abij}}{f_{aa} + f_{bb} - f_{ii} - f_{jj} + G_{abij} + \Delta} \right), \quad (6)$$

$$G_{abij} = \Gamma_{abab} + \Gamma_{ijij} - (\Gamma_{aiai} + \Gamma_{bjbj} + [a \leftrightarrow b]). \quad (7)$$

Here, Δ denotes the energy denominator shift which is introduced to address a known issue in the decoupling of multi-shell Hamiltonian [8]. The issue is that, as the flow parameter s increases, some single-particle levels in the outside space may evolve downward and drop below the valence-space levels [39, 37]. A detailed numerical analysis of the effect of the energy denominator shift Δ can be found in Ref. [8].

It should be noted that the IMSRG evolution induces three- and higher-body terms, which should be kept in principle, but

are computationally impractical. Here we keep up to two-body terms (known as the IMSRG(2) approximation), which has been proven to be an effective many-body truncation when applied to nuclei in different mass regions [33, 55, 56, 53, 57].

As the effective Hamiltonian is obtained in a large model space where conventional shell-model calculations become computationally intractable, we instead exploit the PGCM based on the evolved Hamiltonian $H(s)$. It has been proven to provide a great variational approximation to the conventional shell model [43, 46, 48]. We assume that the many-body wave function can be expressed as a superposition of quantum-number-projected reference states, given by

$$|\Psi_{NZ\sigma}^J\rangle = \sum_{K,q} f_{q,\sigma}^{JK} |JMK; NZ; q\rangle \quad (8)$$

where $|JMK; NZ; q\rangle \equiv \hat{P}_{MK}^J \hat{P}^N \hat{P}^Z |\varphi(q)\rangle$. Here $|\varphi(q)\rangle$ represents a set of intrinsic states obtained by solving the equation of variation after particle-number projection (VAPNP) [58, 59, 60], which is equivalent to determining the Bogoliubov states that are constrained to various amounts of expectation values q for different collective operators and minimize the particle-number-projected energy. In this work we take the operator to be quadrupole moment operator \hat{Q}_{20} since we focus on the enhanced quadrupole collectivity in the island of inversion. \hat{P}' s project intrinsic states onto a well-defined angular momentum J and its z -component M , neutron number N , and proton number Z [61]. $f_{q,\sigma}^{JK}$ is the weight function, where σ is simply an enumeration index. It evaluates the fluctuation of collectivity and can be given by solving the Hill-Wheeler equations [61]:

$$\sum_{K',q'} [\mathcal{H}_{KK'}^J(q, q') - E_{\sigma}^J \mathcal{N}_{KK'}^J(q, q')] f_{q',\sigma}^{JK'} = 0, \quad (9)$$

where the so-called Hamiltonian kernel $\mathcal{H}_{KK'}^J(q; q')$ and the norm kernel $\mathcal{N}_{KK'}^J(q; q')$ are given by

$$\mathcal{H}_{KK'}^J(q, q') = \langle \varphi(q) | H_{\text{eff}} \hat{P}_{KK'}^J \hat{P}^N \hat{P}^Z | \varphi(q') \rangle, \quad (10)$$

$$\mathcal{N}_{KK'}^J(q; q') = \langle \varphi(q) | \hat{P}_{KK'}^J \hat{P}^N \hat{P}^Z | \varphi(q') \rangle. \quad (11)$$

With the PGCM many-body wave function at hand, one can subsequently compute electromagnetic moments and transition probabilities using consistently evolved operators including induced two-body parts [40].

3. Results and discussions

A suitable valence space is of great importance for studying the island of inversion around the neutron number $N = 20$. To evaluate the effect from the extension of valence spaces, we derive effective Hamiltonians in three different valence spaces: the standard sd space above an ^{16}O core, the $sd f_{7/2} p_{3/2}$ space which includes both proton and neutron $0f_{7/2}$ and $1p_{3/2}$ orbits in addition to the sd space, and the $sd fp$ space spanning two full major oscillator shells. For the underlying nuclear interaction, we adopt the 1.8/2.0 (EM) chiral interaction

from Refs. [62, 63, 64], which combines a free-space SRG-evolved NN interaction with an unevolved 3N force. This interaction accurately reproduces the ground-state energies of nuclei up to $A \approx 100$ [41, 57], with a root-mean-square deviation from the experiment of approximately 3.5 MeV across the light- and medium-mass regions [65]. More recently, this interaction has been used to reproduce ground-state energies and spectroscopies of tin isotopes beyond ^{132}Sn within the VS-IMSRG(2) [66]. The IMSRG evolution is carried out in a single particle basis with $e_{\text{max}} = 12$, and 3N matrix elements are truncated at $E_{3\text{max}} = 16$. As the primary application within two-major-shell valence space, we focus on the even-even Ne, Mg, and Si nuclei in vicinity of $N = 20$ in this work.

In multishell valence-space Hamiltonians, whether phenomenologically or microscopically constructed, the issue of center-of-mass (c.m.) contamination must be treated carefully. The Glöckner-Lawson prescription [67] is widely used to remove spurious excited states due to the c.m. motion. Here we exploit the procedure adopted in Ref. [8], that is, add the Glöckner-Lawson term at the beginning of the VS-IMSRG transformation. In this case, the initial Hamiltonian is written as $H = H_{\text{intr}} + \beta H_{\text{c.m.}}$, where H_{intr} denotes the intrinsic Hamiltonian, and $H_{\text{c.m.}} = \mathbf{P}^2/2Am + mA\tilde{\omega}^2 \mathbf{R}^2/2 - 3\hbar\tilde{\omega}/2$ is the c.m. Hamiltonian. Note that β is a scaling parameter and $\tilde{\omega}$ is the frequency of the c.m. Gaussian wave function. The c.m. contamination has been shown to be adequately addressed through this procedure [8]. For further details, see Refs [40, 8]. However, in a large valence space, it is shown that the induced many-body terms of $H_{\text{c.m.}}$ are large, and the IMSRG(2) approximation breaks down in some cases [8]. Therefore, to remove spurious modes due to c.m. motions but not to break the hierarchy of induced terms, we carefully adopt an appropriate β value that keeps these induced terms under control while ensuring that the calculated ground-state energy remains consistent with the experimental data.

In Fig. 1, we compare the low-lying spectra and the reduced $E2$ transition probabilities $B(E2; 0_1^+ \rightarrow 2_1^+)$ of ^{32}Mg calculated in the three model spaces with the experimental data. The calculated g.s. energies are shown in the bottom, compared with the experimental data [68]. Within the full $sd fp$ valence spaces, the g.s. energy decreases by a few MeV. We would expect a slightly more lowered g.s. energy if we can exactly diagonalize the $sd fp$ -shell VS-IMSRG Hamiltonian. Note that the $E2$ transition operators are evolved by the VS-IMSRG transformation consistent with the effective Hamiltonians. We thus avoid ambiguity due to the effective charges. Since we derive the sd -shell effective Hamiltonian from the same 1.8/2.0 (EM) chiral interaction by means of the same IMSRG evolution of Ref. [8], we can benchmark our PGCM calculations with the exact diagonalizations in the sd space. The excitation energy of 2_1^+ state and the $B(E2; 0_1^+ \rightarrow 2_1^+)$ value given by our PGCM calculations are in great agreement with the ones obtained from shell-model calculations [8], which justifies that the PGCM can provide a good approximation to the exact diagonalizations.

Apparently, the calculated 2^+ energy is overestimated and the $B(E2)$ value is underpredicted within the sd valence space. This is consistent with the conclusion that the unexpected enhanced

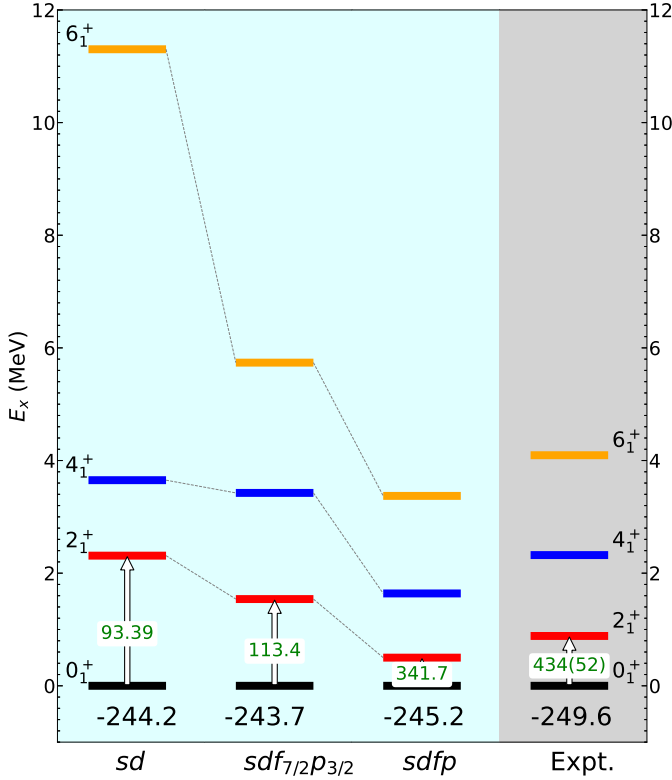


Figure 1: Calculated low-lying spectra of ^{32}Mg obtained within the sd , $sdf_{7/2}p_{3/2}$, and $sdfp$ valence spaces, compared with experimental data. The arrows indicate the $B(E2)$ transition strengths from 0_1^+ to 2_1^+ in units of $e^2\text{fm}^4$. The experimental data are taken from the atomic mass evaluation (AME 2020) [68] and the National Nuclear Data Center (NNDC) [69].

quadrupole collectivity is resulted from the intruder configurations of the fp shell. As we expand the valence space, the excitation energies of the yrast 2_1^+ , 4_1^+ , and 6_1^+ states are lowered. Within the full $sdfp$ shell, the calculated low-lying states exhibit an evident rotational behavior, in reasonably good agreement with the experimental data. The suppression of 2^+ energy implies an increase in quadrupole collectivity due to the intruder configurations of the fp shell. Moreover, the reduced $E2$ transition strength $B(E2; 0_1^+ \rightarrow 2_1^+)$ provides a direct probe to the quadrupole collectivity. As indicated by the arrows in Fig. 1, the calculated $B(E2; 0_1^+ \rightarrow 2_1^+)$ values increase substantially with the inclusion of more orbitals and tend to reproduce the adopted value [70]. The $B(E2; 0_1^+ \rightarrow 2_1^+)$ obtained within the full $sdfp$ space is $341.7 e^2\text{fm}^4$, which is compatible with the shell-model result employed a $sdfp$ -shell effective Hamiltonian derived from the EKK method and the effective charges $(e_p, e_n) = (1.25, 0.25)e$ [4]. Here we emphasize that our VS-IMSRG+PGCM calculations do not fit the single-particle energies or introduce the assumption of effective charges. Although the calculated $B(E2)$ is significantly improved compared to the VS-IMSRG calculations within smaller valence spaces, it is still a bit smaller than the adopted value. The VS-IMSRG has been found to systematically underestimate the $B(E2)$ values in well-deformed nuclei when truncated at the normal-ordered two-body (NO2B) [40, 71, 8, 72]. Moreover, we have attempted

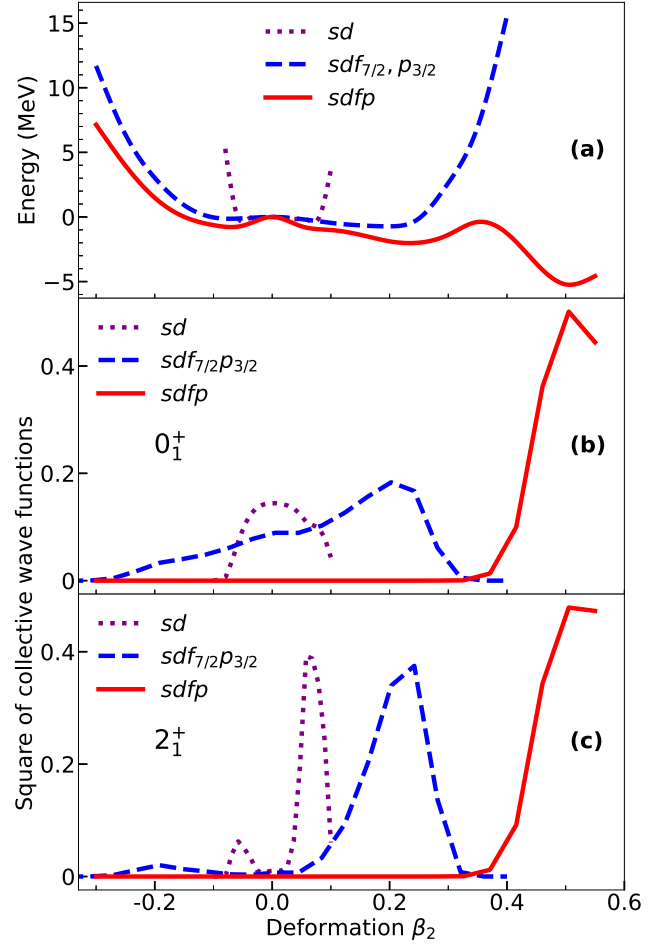


Figure 2: (a) Projected potential energy of ^{32}Mg with particle-number projection and angular-momentum projection onto $J = 0$ against axial deformation β_2 , calculated in the sd , $sdf_{7/2}p_{3/2}$, and $sdfp$ spaces. For clarity, the spherical configuration energy has been set to zero. (b) The distributions of collective wavefunction of 0_1^+ state in 3 different model spaces. (c) Same as panel (b) but for 2_1^+ states.

to further expand the valence space to include the neutron $0g_{9/2}$ shell. We found that the procedure of c.m. factorization spoiled the hierarchy of the induced many-body terms, resulting in the ground-state energy drops rapidly. This presents a new challenge in the decoupling procedure of multishell Hamiltonians.

It is intriguing to see the evolution of nuclear quadrupole deformation with gradual expansion of valence spaces and its impact on the low-lying structure of ^{32}Mg . Figure 2(a) illustrates the projected potential energy of ^{32}Mg against the axial quadrupole deformation β_2 calculated within the three different valence spaces, all with projection of particle number onto $Z = 12$ and $N = 20$, and angular momentum onto $J = 0$. As the model spaces expand, the projected potential energy curves (PECs) span a wider range of nuclear quadrupole deformation. It is because the inclusion of high- j orbits allows stronger quadrupole correlations and thus generates larger deformations. The minimum shifts from near-sphericity within the sd space to a large prolate deformation of $\beta_2 \approx 0.5$ within

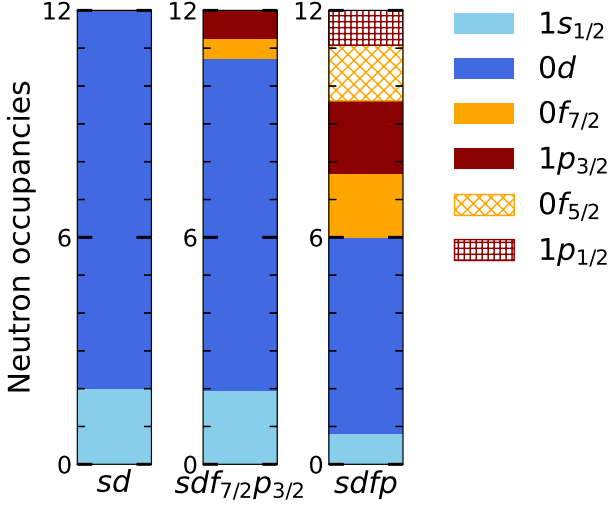


Figure 3: Neutron occupancies calculated within the sd , $sdf_{7/2}p_{3/2}$, and $sdfp$ spaces. Note that “ $1d$ ” denotes for neutrons occupied the $1d_{5/2}$ and $1d_{3/2}$ orbitals.

the $sdfp$ space. Note that our $sdfp$ -shell projected PEC is strikingly similar to the projected PEC given by IM-GCM employing a Hamiltonian appropriately evolved by MR-IMSRG [25], although the limited valence space in our calculations prevents constraining to larger deformations of $\beta_2 \geq 0.6$.

In addition, we show the distribution of collective wave functions for the 0^+ ground state and the 2^+_1 excited state computed within three valence spaces in Fig. 2(b) and Fig. 2(c), respectively. The distribution of collective wave functions is defined to account for the probability density, normalized to 1, of finding the state $|\Psi_{NZ\sigma}^J\rangle$ with given deformation parameters β_2 (see more details in Refs. [73, 74]). One can see that the 0^+_1 and 2^+_1 states obtained within the sd space are dominated by near-spherical configurations with $|\beta_2| \leq 0.08$. In contrast, the distribution of the 0^+_1 state within the $sdf_{7/2}p_{3/2}$ space exhibits a remarkable mixture of moderately prolate and oblate deformed configurations spanning in the region with $|\beta_2| \leq 0.3$, which is compatible with the projected PEC that two shallow minima appear at prolate and oblate side. Finally, in the $sdfp$ model space, the 0^+_1 and 2^+_1 states are predominated by strongly prolate deformed configurations with $\beta_2 \approx 0.5$, indicating a significantly more deformed state. The distribution of collective wave functions clearly demonstrates that dominant configurations gradually shift toward stronger quadrupole collectivity along with the expansion of the valence space, thereby highlighting the necessity of employing two-major-shell valence space to fully capture the enhanced collectivity of island of inversion.

Previous studies suggested that the onset of enhanced quadrupole collectivity is due to mp - mh excitation over the $N = 20$ shell gap for the ground state. Fig 3 depicts the neutron occupancies obtained with the VS-IMSRG Hamiltonians decoupled to three valence spaces. It demonstrates that, as we gradually expand the valence spaces, more neutrons in-

tend to excite from the sd to the fp shells. Note that our VS-IMSRG+PGCM result within the $sdf_{7/2}p_{3/2}$ space shows that ~ 1.5 neutrons occupy the fp shell, which is compatible with the previous $\pi sd + \nu sdf_{7/2}p_{3/2}$ shell VS-IMSRG calculation [8]. Within the full $sdfp$ space, more neutrons are promoted to the fp shell. Inclusion of neutron $0f_{5/2}$ and $1p_{1/2}$ orbitals not only allows neutrons to excite and occupy these two orbitals, but also enhances the occupation of the $0f_{7/2}$ and $1p_{3/2}$ orbitals. It may imply that the IMSRG decoupling to larger valence space captures more dynamical correlations associated with high-energy multi-particle multi-hole (mp - mh) excitations. Fig 3, combined with Fig 1, indicates the correlation between the onset of enhanced quadrupole collectivity and the cross-shell mp - mh excitations, as well as the importance of larger valence spaces.

We broaden our calculations to investigate the low-lying states of $^{30,34}\text{Mg}$ and the $N = 20$ isotones ^{30}Ne and ^{34}Si , using the *ab initio* $sdfp$ -shell Hamiltonians derived from VS-IMSRG. The calculated g.s. energies, level spectra and $B(E2; 0^+_1 \rightarrow 2^+_1)$ values are compared with the experimental data in Fig. 4. For all investigated nuclei, our calculations reproduce the observations reasonably well, whereas the previous VS-IMSRG calculations within smaller model spaces systematically overestimated the 2^+_1 excitation energies and underestimated the $B(E2; 0^+_1 \rightarrow 2^+_1)$ values [8]. As the neutron numbers increase in the Mg isotopes, the calculated excitation energies of the 2^+_1 states show a notable lowering at $N = 20$. Although the calculations exaggerate the lowering in a certain context, it is in accordance with the experimental trend. Also, the $B(E2)$ values increase along with the neutron numbers around $N = 20$ for Mg isotopes, exhibiting the disappearance of $N = 20$ shell gap and the formation of the island of inversion.

For $N = 20$ isotones, our $sdfp$ -shell calculations give a moderate lowering of 2^+_1 energy and a slight enhancement of $B(E2; 0^+_1 \rightarrow 2^+_1)$ value for ^{30}Ne compared to the previous $\pi sd + \nu sdf_{7/2}p_{3/2}$ shell VS-IMSRG calculations [8], improving the agreement. In contrast, the calculated 2^+_1 energy of ^{34}Si is much higher than that of ^{30}Ne and ^{32}Mg , and the $B(E2)$ value is significantly lower. It indicates the predominant role of the spherical configuration in the 0^+_1 ground state and the 2^+_1 excited state of ^{34}Si . Note that our $sdfp$ -shell calculations reproduce well the observed 2^+_1 energy of ^{34}Si , but give a $B(E2; 0^+_1 \rightarrow 2^+_1)$ value smaller than the adopt value. This may be attributed to the fact that the *ab initio* methods based on spherical references tend to underestimate $B(E2)$ values due to missing contributions from mp - mh excitations [8, 40, 71]. Combining 2^+_1 energies and $B(E2)$, we demonstrate an apparent collapse of the $N = 20$ shell closure in the ^{30}Ne and ^{32}Mg and its persistence in ^{34}Si . Overall, we found that the VS-IMSRG+PGCM within the full two-major-shell valence space provides a reasonably good description of the border of the island of inversion.

The neutron occupancies computed within the full $sdfp$ space for the ground states of ^{30}Ne , $^{30-34}\text{Mg}$, and ^{34}Si are summarized in Fig. 4, illustrating the evolution of cross-shell mp - mh excitation along the isotopic and isotonic chains. For $^{30-34}\text{Mg}$, we see a sudden jump in neutron occupancies of the fp shell at $N = 20$. It is consistent with the earlier phenomenological shell model studies [13, 3], the empirical analysis given

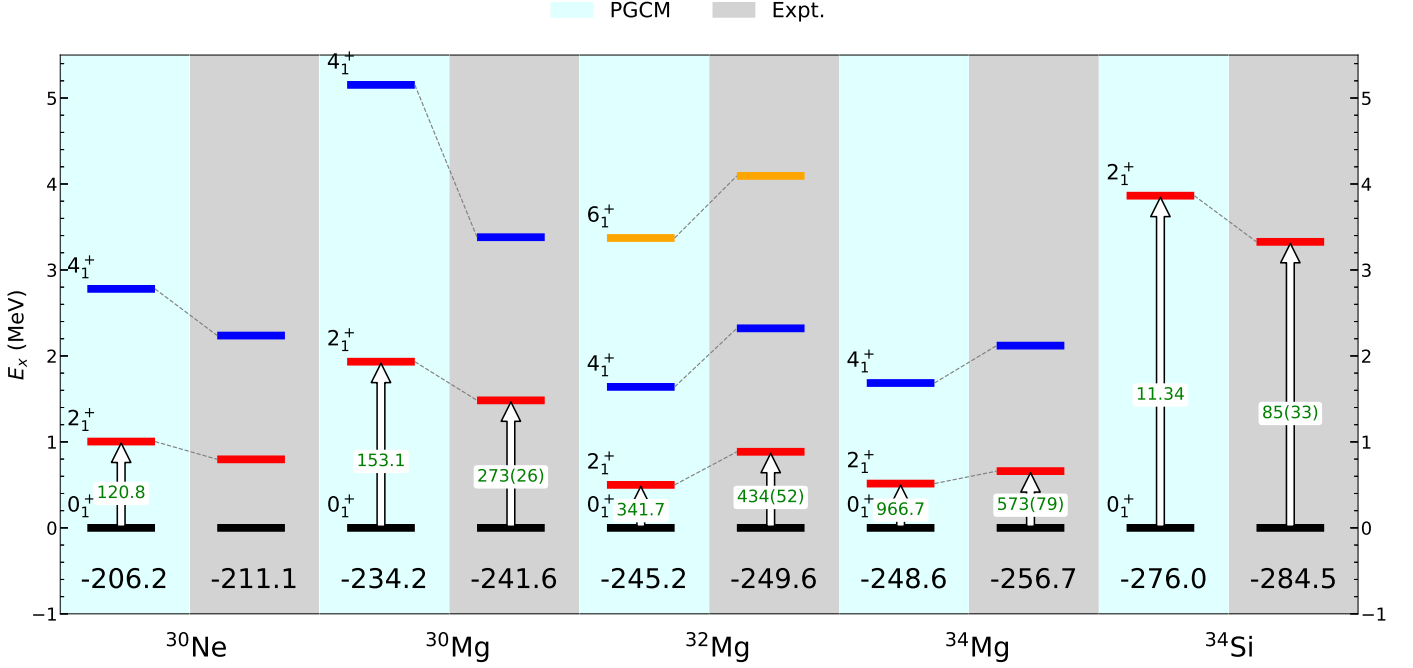


Figure 4: Calculated low-lying spectra of ^{30}Ne , $^{30-34}\text{Mg}$, and ^{34}Si within *sdfp* model space, compared with the experimental data. The arrows indicate the $B(E2; 0_1^+ \rightarrow 2_1^+)$ values in units of $e^2 fm^4$. The experimental data are taken from the AME 2020 [68] and NNDC [69]. The calculations are done with $e_{max} = 12$ and $E_{3max} = 16$.

by a three-level mixing model [75], and the VS-IMSRG study within smaller valence spaces [8]. A further moderate increase in neutron occupancies of the *fp* shell is presented for ^{34}Mg . For $N = 20$ isotones, about 2 neutrons are excited to the *fp* shell in the ground state of ^{30}Ne , which corresponds to the conventional picture of being a $2p - 2h$ state. In contrast, the ground state of ^{34}Si is shown to be dominated by neutrons occupying the *sd* shell, clearly indicating the persistence of the $N = 20$ shell closure. We note that our calculation overpredicts the *fp*-shell occupancies for $^{32,34}\text{Mg}$ when compared to the conventional picture for ^{32}Mg being basically a $2p-2h$ state, as suggested by phenomenological shell-model studies [76, 13, 3]. This may be attributed to the fact that dynamical correlations from particle-hole excitations are incorporated into the effective Hamiltonian by the VS-IMSRG evolution. Note that the semi-microscopic MBPT approach employed the EKK method [4] and the empirical three-level mixing model [75] also suggested the large probability of higher *mp-mh* configurations in the 0_1^+ state of ^{32}Mg . Also, the occupation numbers are model-dependent, and so calculations employing different Hamiltonians need not agree on them. Therefore, no strong conclusions should be drawn here.

Finally, it is of particular interest to compare the low-lying spectroscopies given by our VS-IMSRG+PGCM framework with that obtained from the IM-GCM calculations [25] which combines the PGCM with the MR-IMSRG rather than the VS-IMSRG. We note the striking similarity between the projected PEC's obtained with these two methods. Both approaches consistently reproduce the observed onset of large quadrupole collectivity from ^{30}Mg to ^{34}Mg indicated by the compression of the low-lying rotational bands and the increase

in $B(E2; 0_1^+ \rightarrow 2_1^+)$. Our VS-IMSRG+PGCM calculations present slightly compressed level spectra for $^{32,34}\text{Mg}$ when compared to the experimental data, whereas the IM-GCM ones are somewhat stretched. Moreover, the IM-GCM quantitatively reproduces the adopted $B(E2; 0_1^+ \rightarrow 2_1^+)$ values within the experimental errors, while our VS-IMSRG+PGCM calculations still slightly underpredict the $B(E2; 0_1^+ \rightarrow 2_1^+)$ values for ^{30}Mg and ^{32}Mg . This underestimation of the electromagnetic transition strengths, despite remarkably improvement through expanding the valence spaces, may be attributed to normal ordering with respect to an ensemble of spherical reference states rather than an ensemble of multiple symmetry-restored Hartree-Fock-Bogoliubov states that are used in the IM-GCM [25].

4. Summary and conclusions

In this work, we have extended the VS-IMSRG framework to decouple the *ab initio* multishell valence space Hamiltonians connecting two major-oscillator *sdfp* shells, starting from chiral *NN* and *3N* forces. To handle the effective Hamiltonians within large valence spaces, we employed the PGCM variationally approximate the conventional shell model. Without further empirical fitting and assumption of effective charges, we study the nuclear spectroscopy of strongly deformed open-shell nuclei in the island of inversion around $N = 20$. The expanded model space markedly improves the description of collective properties, e.g., excitation energies of 2^+ states and $E2$ transition strengths in nuclei inside or outside of the island of inversion, confirming the disappearance of the $N = 20$ shell closure and the onset of intruder configurations driven by cross-shell *mp-mh* correlations. The calculated neutron occupancies,

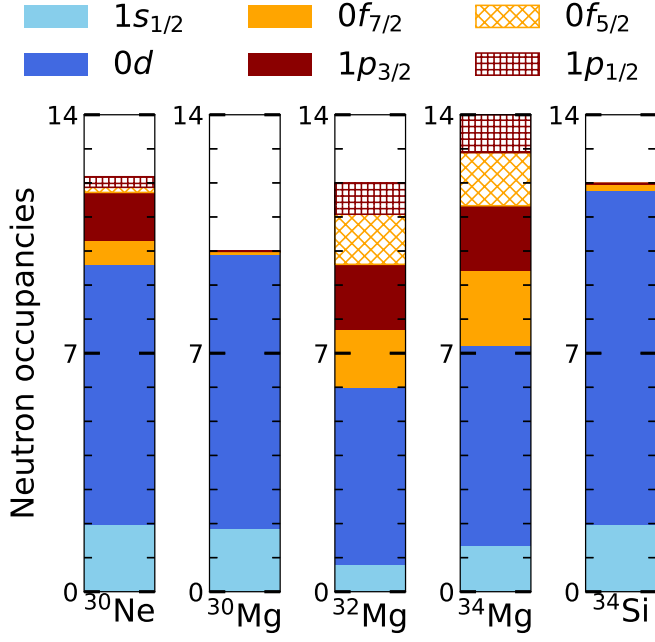


Figure 5: Neutron occupancies calculated within the full $sdfp$ space for the ground states of $^{30-34}\text{Mg}$ and the adjacent $N = 20$ isotones ^{30}Ne , ^{34}Si . Note that “ $0d$ ” denotes for neutrons occupied the $0d_{5/2}$ and $0d_{3/2}$ orbitals.

which depicts the intruder configurations arising from the mp - mh excitations across the $N = 20$ shell gap, are consistent with the conclusions of the phenomenological studies.

The reasonably good description of the island of inversion reveals that, within suitable multishell valence spaces, the VS-IMSRG is capable of sufficiently incorporating dynamical correlations associated with high-energy mp - mh excitations into the effective Hamiltonian, while static (or collective) correlations, such as pairing and deformation, are essentially captured via the PGCM. Since the VS-IMSRG+PGCM approach allows us to add or remove the valence orbits and collective coordinates, we can elucidate the essential degrees of freedom for describing a many-body wave function. While we need to carefully check the center-of-mass contamination when we choose an appropriate multishell valence space, this method provides us with an opportunity for *ab initio* valence-space-based studies with tractable computational cost on the heavier open-shell nuclei, in which nucleons are strongly correlated.

Acknowledgements

The authors would like to thank J. M. Yao for fruitful discussions and useful comments. We thank T. Miyagi for the NuHamil [77] which was used to generate chiral EFT matrix elements, and R. Stroberg for the IMSRG++ [78] which was used to perform the VS-IMSRG decoupling. The authors also thank B. Bally and T. R. Rodríguez since the PGCM code was developed based on the TAURUS [79, 80]. This material is based on the work supported by the National Natural Science Foundation of China under Grant No. 12275369.

References

- [1] M. G. Mayer, On closed shells in nuclei. ii, Phys. Rev. 75 (1949) 1969–1970. doi:10.1103/PhysRev.75.1969. URL <https://link.aps.org/doi/10.1103/PhysRev.75.1969>.
- [2] O. Haxel, J. H. D. Jensen, H. E. Suess, On the “magic numbers” in nuclear structure, Phys. Rev. 75 (1949) 1766–1766. doi:10.1103/PhysRev.75.1766.2. URL <https://link.aps.org/doi/10.1103/PhysRev.75.1766.2>.
- [3] E. Caurier, F. Nowacki, A. Poves, Merging of the islands of inversion at $n = 20$ and $n = 28$, Phys. Rev. C 90 (2014) 014302. doi:10.1103/PhysRevC.90.014302. URL <https://link.aps.org/doi/10.1103/PhysRevC.90.014302>.
- [4] N. Tsunoda, T. Otsuka, N. Shimizu, M. Hjorth-Jensen, K. Takayanagi, T. Suzuki, Exotic neutron-rich medium-mass nuclei with realistic nuclear force, Phys. Rev. C 95 (2017) 021304. doi:10.1103/PhysRevC.95.021304. URL <https://link.aps.org/doi/10.1103/PhysRevC.95.021304>.
- [5] E. Caurier, G. Martínez-Pinedo, F. Nowacki, A. Poves, A. P. Zuker, The shell model as a unified view of nuclear structure, Rev. Mod. Phys. 77 (2005) 427–488. doi:10.1103/RevModPhys.77.427. URL <https://link.aps.org/doi/10.1103/RevModPhys.77.427>.
- [6] T. Otsuka, A. Gade, O. Sorlin, T. Suzuki, Y. Utsuno, Evolution of shell structure in exotic nuclei, Rev. Mod. Phys. 92 (2020) 015002. doi:10.1103/RevModPhys.92.015002. URL <https://link.aps.org/doi/10.1103/RevModPhys.92.015002>.
- [7] N. Tsunoda, T. Otsuka, K. Takayanagi, N. Shimizu, T. Suzuki, Y. Utsuno, S. Yoshida, H. Ueno, The impact of nuclear shape on the emergence of the neutron drip line, Nature 587 (7832) (2020) 66–71. doi:10.1038/s41586-020-2848-x. URL <https://doi.org/10.1038/s41586-020-2848-x>.
- [8] T. Miyagi, S. R. Stroberg, J. D. Holt, N. Shimizu, Ab initio multishell valence-space hamiltonians and the island of inversion, Phys. Rev. C 102 (2020) 034320. doi:10.1103/PhysRevC.102.034320. URL <https://link.aps.org/doi/10.1103/PhysRevC.102.034320>.
- [9] E. K. Warburton, J. A. Becker, B. A. Brown, Mass systematics for $a=29-44$ nuclei: The deformed $a\sim 32$ region, Phys. Rev. C 41 (1990) 1147–1166. doi:10.1103/PhysRevC.41.1147. URL <https://link.aps.org/doi/10.1103/PhysRevC.41.1147>.
- [10] T. Motobayashi, Y. Ikeda, K. Ieki, M. Inoue, N. Iwasa, T. Kikuchi, M. Kurokawa,

- S. Moriya, S. Ogawa, H. Murakami, S. Shimoura, Y. Yanagisawa, T. Nakamura, Y. Watanabe, M. Ishihara, T. Teranishi, H. Okuno, R. Casten, **Large deformation of the very neutron-rich nucleus ^{32}Mg from intermediate-energy collision of ^{33}Mg ; Evidence for a negative-parity 0^+ state in ^{32}Mg** , *Phys. Rev. Lett.* **99** (2007) 212501. doi:<https://doi.org/10.1103/PhysRevLett.99.212501>. URL <https://www.sciencedirect.com/science/article/pii/S0370269306001248>.
- [11] C. Thibault, R. Klapisch, C. Rigaud, A. M. Poskanzer, R. Prieels, L. Lessard, W. Reisdorf, **Direct measurement of the masses of ^{11}Li and $^{26-32}\text{Na}$ with an on-line mass separator**, *Phys. Rev. C* **12** (1975) 644–657. doi:[10.1103/PhysRevC.12.644](https://doi.org/10.1103/PhysRevC.12.644). URL <https://link.aps.org/doi/10.1103/PhysRevC.12.644>.
- [12] T. Otsuka, T. Suzuki, R. Fujimoto, H. Grawe, Y. Akaishi, **Evolution of nuclear shells due to the tensor force**, *Phys. Rev. Lett.* **95** (2005) 232502. doi:[10.1103/PhysRevLett.95.232502](https://doi.org/10.1103/PhysRevLett.95.232502). URL <https://link.aps.org/doi/10.1103/PhysRevLett.95.232502>.
- [13] Y. Utsuno, T. Otsuka, T. Mizusaki, M. Honma, **Varying shell gap and deformation in $n \sim 20$ unstable nuclei studied by the monte carlo shell model**, *Phys. Rev. C* **60** (1999) 054315. doi:[10.1103/PhysRevC.60.054315](https://doi.org/10.1103/PhysRevC.60.054315). URL <https://link.aps.org/doi/10.1103/PhysRevC.60.054315>.
- [14] A. Poves, J. Retamosa, **The onset of deformation at the $n = 20$ neutron shell closure far from stability**, *Phys. Rev. Lett.* **184** (4) (1987) 311–315. doi:[https://doi.org/10.1016/0370-2693\(87\)90171-7](https://doi.org/10.1016/0370-2693(87)90171-7). URL <https://www.sciencedirect.com/science/article/pii/S0370269387901717>.
- [15] C. Détraz, D. Guillemaud, G. Huber, R. Klapisch, M. Langevin, F. Naulin, C. Thibault, L. Carraz, F. Touchard, **Beta decay of $^{27-32}\text{Na}$ and their descendants**, *Phys. Rev. C* **19** (1979) 164–176. doi:[10.1103/PhysRevC.19.164](https://doi.org/10.1103/PhysRevC.19.164). URL <https://link.aps.org/doi/10.1103/PhysRevC.19.164>.
- [16] D. Guillemaud-Mueller, C. Détraz, M. Langevin, F. Naulin, M. de Saint-Simon, C. Thibault, F. Touchard, M. Epherre, **β -decay schemes of very neutron-rich sodium isotopes and their descendants**, *Nuclear Physics A* **426** (1) (1984) 37–76. doi:[https://doi.org/10.1016/0375-9474\(84\)90064-2](https://doi.org/10.1016/0375-9474(84)90064-2). URL <https://www.sciencedirect.com/science/article/pii/0375947484900642>.
- [17] H. Iwasaki, T. Motobayashi, H. Sakurai, K. Yoneda, T. Gomi, N. Aoi, N. Fukuda, Z. Fülöp, U. Futakami, Z. Gacsi, Y. Higurashi, N. Imai, N. Iwasa, T. Kubo, M. Kunibu, M. Kurokawa, Z. Liu, T. Minemura, A. Saito, M. Serata, S. Shimoura, S. Takeuchi, Y. Watanabe, K. Yamada, Y. Yanagisawa, M. Ishihara, **Large collectivity of ^{34}Mg** , *Phys. Rev. Lett.* **522** (3) (2001) 227–232. doi:[https://doi.org/10.1016/S0370-2693\(01\)01244-8](https://doi.org/10.1016/S0370-2693(01)01244-8). URL <https://www.sciencedirect.com/science/article/pii/S0370269301012448>.
- [18] D. T. Yordanov, M. Kowalska, K. Blaum, M. De Rydt, K. T. Flanagan, P. Lievens, R. Neugart, G. Neyens, H. H. Stroke, **Spinel-magnetron ion beam of ^{33}Mg ; Evidence for a negative-parity 0^+ state in ^{32}Mg** , *Phys. Rev. Lett.* **99** (2007) 212501. doi:[10.1103/PhysRevLett.99.212501](https://doi.org/10.1103/PhysRevLett.99.212501). URL <https://link.aps.org/doi/10.1103/PhysRevLett.99.212501>.
- [19] K. Wimmer, T. Kröll, R. Krücken, V. Bildstein, R. Gernhäuser, B. Bastin, N. Bree, J. Diriken, R. Van Duppen, M. Huyse, N. Patronis, P. Vermaelen, D. Voulot, J. Van de Walle, F. Wenander, L. M. Fraile, R. Chapman, B. Hadinia, R. Orlandi, F. Smith, R. Lutter, P. G. Thirolf, M. Labiche, A. Blazhev, M. Kalkühler, P. Reiter, M. Seidlitz, N. Warr, A. O. Macchiavelli, H. B. Jeppesen, E. Fiori, G. Georgiev, G. Schrieder, S. Das Gupta, G. Lo Bianco, S. Nardelli, J. Butterworth, J. Johansen, K. Riisager, **Discovery of the shape coexisting 0^+ state in ^{32}Mg by a two neutron transfer reaction**, *Phys. Rev. Lett.* **105** (2010) 252501. doi:[10.1103/PhysRevLett.105.252501](https://doi.org/10.1103/PhysRevLett.105.252501). URL <https://link.aps.org/doi/10.1103/PhysRevLett.105.252501>.
- [20] P. Doornenbal, H. Scheit, S. Takeuchi, N. Aoi, K. Li, M. Matsushita, D. Steppenbeck, H. Wang, H. Baba, H. Crawford, C. R. Hoffman, R. Hughes, E. Ideguchi, N. Kobayashi, Y. Kondo, J. Lee, S. Michimasa, T. Motobayashi, H. Sakurai, M. Takechi, Y. Togano, R. Winkler, K. Yoneda, **In-beam γ -ray spectroscopy of $^{34,36}\text{Mg}$: Merging the $n=20$ and $n=28$ shell closures**, *Phys. Rev. Lett.* **111** (2013) 212502. doi:[10.1103/PhysRevLett.111.212502](https://doi.org/10.1103/PhysRevLett.111.212502). URL <https://link.aps.org/doi/10.1103/PhysRevLett.111.212502>.
- [21] P. Doornenbal, H. Scheit, S. Takeuchi, N. Aoi, K. Li, M. Matsushita, D. Steppenbeck, H. Wang, H. Baba, E. Ideguchi, N. Kobayashi, Y. Kondo, J. Lee, S. Michimasa, T. Motobayashi, A. Poves, H. Sakurai, M. Takechi, Y. Togano, K. Yoneda, **Mapping the deformation in the “island of inversion”: Inelastic scattering of ^{34}Mg on ^{208}Pb** , *Phys. Rev. C* **93** (2016) 044306. doi:[10.1103/PhysRevC.93.044306](https://doi.org/10.1103/PhysRevC.93.044306). URL <https://link.aps.org/doi/10.1103/PhysRevC.93.044306>.
- [22] X. Campi, H. Flocard, A. Kerman, S. Koonin, **Shape transition in the neutron rich sodium isotopes**, *Nuclear Physics A* **251** (2) (1975) 193–205. doi:[https://doi.org/10.1016/0375-9474\(75\)90065-2](https://doi.org/10.1016/0375-9474(75)90065-2). URL <https://www.sciencedirect.com/science/article/pii/0375947475900652>.
- [23] E. Caurier, F. Nowacki, A. Poves, J. Retamosa, **Shell model study of the neutron rich isotopes from oxygen to silicon**, *Phys. Rev. C* **58** (1998) 2033–2040. doi:[10.1103/PhysRevC.58.2033](https://doi.org/10.1103/PhysRevC.58.2033). URL <https://link.aps.org/doi/10.1103/PhysRevC.58.2033>.
- [24] M. Yamagami, N. Van Giai, **Pairing effects on the collectivity of quadrupole states around ^{32}Mg** , *Phys. Rev. C* **69** (2004) 034301. doi:<https://doi.org/10.1103/PhysRevC.69.034301>. URL <https://link.aps.org/doi/10.1103/PhysRevC.69.034301>.

- doi:10.1103/PhysRevC.69.034301.
URL <https://link.aps.org/doi/10.1103/PhysRevC.69.034301>.
- [25] E. Zhou, C. Ding, J. Yao, B. Bally, H. Hergert, C. Jiao, T. Rodríguez, *Ab initio nuclear shape coexistence and emergence of island of inversion in ^{132}Xe* , *Physics Letters B* 865 (2025) 139464.
doi:10.1016/j.physletb.2025.139464.
URL <https://www.sciencedirect.com/science/article/pii/S0370269325002254>.
- [26] D. Lee, *Lattice simulations for few- and many-body systems*, *Progress in Particle and Nuclear Physics* 63 (1) (2009) 117–154.
doi:10.1016/j.ppnp.2008.12.001.
URL <https://www.sciencedirect.com/science/article/pii/S014664100800094X>.
- [27] P. Navrátil, S. Quaglioni, I. Stetcu, B. R. Barrett, *Recent developments in no-core shell-model calculations*, *Journal of Physics G: Nuclear and Particle Physics* 36 (8) (2009) 083101.
doi:10.1088/0954-3899/36/8/083101.
URL <https://dx.doi.org/10.1088/0954-3899/36/8/083101>.
- [28] B. R. Barrett, P. Navrátil, J. P. Vary, *Ab initio no core shell model*, *Progress in Particle and Nuclear Physics* 69 (2013) 131–181.
doi:10.1016/j.ppnp.2012.10.003.
URL <https://www.sciencedirect.com/science/article/pii/S0146641012001184>.
- [29] V. Somà, A. Cipollone, C. Barbieri, P. Navrátil, T. Duguet, *Chiral two- and three-nucleon forces along medium-mass isotope chains*, *Phys. Rev. C* 89 (2014) 061301.
doi:10.1103/PhysRevC.89.061301.
URL <https://link.aps.org/doi/10.1103/PhysRevC.89.061301>.
- [30] G. Hagen, T. Papenbrock, M. Hjorth-Jensen, D. J. Dean, *Coupled-cluster computations of atomic nuclei*, *Reports on Progress in Physics* 77 (9) (2014) 096302.
doi:10.1088/0034-4885/77/9/096302.
URL <https://dx.doi.org/10.1088/0034-4885/77/9/096302>.
- [31] J. Carlson, S. Gandolfi, F. Pederiva, S. C. Pieper, R. Schiavilla, K. E. Schmidt, R. B. Wiringa, *Quantum monte carlo methods for nuclear physics*, *Rev. Mod. Phys.* 87 (2015) 1067–1118.
doi:10.1103/RevModPhys.87.1067.
URL <https://link.aps.org/doi/10.1103/RevModPhys.87.1067>.
- [32] K. D. Launey, T. Dytrych, J. P. Draayer, *Symmetry-guided large-scale shell-model theory*, *Progress in Particle and Nuclear Physics* 89 (2016) 101–136.
doi:10.1016/j.ppnp.2016.02.001.
URL <https://www.sciencedirect.com/science/article/pii/S0146641016000338>.
- [33] H. Hergert, S. Bogner, T. Morris, A. Schwenk, K. Tsukiyama, *The in-medium similarity renormalization group: A novel ab initio method for nuclei*, *Physics Reports* 621 (2016) 165–222, memorial Volume in Honor of Gerald E. Brown.
- [34] S. Weinberg, *Effective chiral lagrangians for nucleon-pion interactions*, *Nuclear Physics B* 363 (1) (1991) 3–18.
doi:10.1016/0550-3213(91)90231-L.
URL <https://www.sciencedirect.com/science/article/pii/S055032139190231L>.
- [35] R. Machleidt, D. Entem, *Chiral effective field theory and nuclear forces*, *Physics Reports* 503 (1) (2011) 1–75.
doi:10.1016/j.physrep.2011.02.001.
URL <https://www.sciencedirect.com/science/article/pii/S037026931000094X>.
- [36] E. Epelbaum, H.-W. Hammer, U.-G. Meißner, *Modern theory of nuclear forces*, *Rev. Mod. Phys.* 81 (2009) 1773–1825.
doi:10.1103/RevModPhys.81.1773.
URL <https://link.aps.org/doi/10.1103/RevModPhys.81.1773>.
- [37] S. R. Stroberg, A. Calci, H. Hergert, J. D. Holt, S. K. Bogner, R. Roth, A. Schwenk, *Nucleus-dependent valence-space approach to nuclear structure*, *Phys. Rev. Lett.* 118 (2017) 032502.
doi:10.1103/PhysRevLett.118.032502.
URL <https://link.aps.org/doi/10.1103/PhysRevLett.118.032502>.
- [38] S. K. Bogner, H. Hergert, J. D. Holt, A. Schwenk, S. Binder, A. Calci, J. Langhammer, R. Roth, *Nonperturbative shell-model interactions from the in-medium similarity renormalization group*, *Phys. Rev. Lett.* 113 (2014) 142501.
doi:10.1103/PhysRevLett.113.142501.
URL <https://link.aps.org/doi/10.1103/PhysRevLett.113.142501>.
- [39] S. R. Stroberg, H. Hergert, J. D. Holt, S. K. Bogner, A. Schwenk, *Ground and excited states of doubly open-shell nuclei from ab initio calculations*, *Phys. Rev. C* 93 (2016) 051301.
doi:10.1103/PhysRevC.93.051301.
URL <https://link.aps.org/doi/10.1103/PhysRevC.93.051301>.
- [40] N. M. Parzuchowski, S. R. Stroberg, P. Navrátil, H. Hergert, S. K. Bogner, *Ab initio electromagnetic observables with the in-medium similarity renormalization group*, *Phys. Rev. C* 96 (2017) 034324.
doi:10.1103/PhysRevC.96.034324.
URL <https://link.aps.org/doi/10.1103/PhysRevC.96.034324>.
- [41] S. R. Stroberg, H. Hergert, S. K. Bogner, J. D. Holt, *Nonempirical interactions for the nuclear shell model: An update*, *Annual Review of Nuclear and Particle Science* 69 (Volume 69, 2019) (2019) 307–362.
doi:10.1146/annurev-nucl-101917-021146.
URL <https://www.annualreviews.org/content/journals/10.1146/annurev-nucl-101917-021146>.
- [42] S. Sahoo, P. C. Srivastava, *Ab initio study of the island of inversion in odd- A nuclei: Structure and spectroscopy*, *Phys. Rev. C* 111 (2025) 054308.
doi:10.1103/PhysRevC.111.054308.
URL <https://link.aps.org/doi/10.1103/PhysRevC.111.054308>.

- [43] C. F. Jiao, J. Engel, J. D. Holt, [doi:10.1103/PhysRevC.96.054310](https://doi.org/10.1103/PhysRevC.96.054310), [Phys. Rev. C](https://link.aps.org/doi/10.1103/PhysRevC.96.054310) **96** (2017) 054310. URL <https://link.aps.org/doi/10.1103/PhysRevC.96.054310>.
- [44] C. F. Jiao, M. Horoi, A. Neacsu, [doi:10.1103/PhysRevC.98.064324](https://doi.org/10.1103/PhysRevC.98.064324), [Phys. Rev. C](https://link.aps.org/doi/10.1103/PhysRevC.98.064324) **98** (2018) 064324. URL <https://link.aps.org/doi/10.1103/PhysRevC.98.064324>.
- [45] J. M. Yao, J. Engel, L. J. Wang, C. F. Jiao, H. Hergert, [doi:10.1103/PhysRevC.98.054311](https://doi.org/10.1103/PhysRevC.98.054311), [Phys. Rev. C](https://link.aps.org/doi/10.1103/PhysRevC.98.054311) **98** (2018) 054311. URL <https://link.aps.org/doi/10.1103/PhysRevC.98.054311>.
- [46] B. Bally, A. Sánchez-Fernández, T. R. Rodríguez, [doi:10.1103/PhysRevC.100.044308](https://doi.org/10.1103/PhysRevC.100.044308), [Phys. Rev. C](https://link.aps.org/doi/10.1103/PhysRevC.100.044308) **100** (2019) 044308. URL <https://link.aps.org/doi/10.1103/PhysRevC.100.044308>.
- [47] C. Jiao, C. W. Johnson, [doi:10.1103/PhysRevC.100.031303](https://doi.org/10.1103/PhysRevC.100.031303), [Phys. Rev. C](https://link.aps.org/doi/10.1103/PhysRevC.100.031303) **100** (2019) 031303. URL <https://link.aps.org/doi/10.1103/PhysRevC.100.031303>.
- [48] N. Shimizu, T. Mizusaki, K. Kaneko, Y. Tsunoda, [doi:10.1103/PhysRevC.103.064302](https://doi.org/10.1103/PhysRevC.103.064302), [Phys. Rev. C](https://link.aps.org/doi/10.1103/PhysRevC.103.064302) **103** (2021) 064302. URL <https://link.aps.org/doi/10.1103/PhysRevC.103.064302>.
- [49] G. Hagen, S. J. Novario, Z. H. Sun, T. Papenbrock, G. R. Jansen, J. G. Lietz, T. Duguet, A. Tichai, [doi:10.1103/PhysRevC.105.064311](https://doi.org/10.1103/PhysRevC.105.064311), [Phys. Rev. C](https://link.aps.org/doi/10.1103/PhysRevC.105.064311) **105** (2022) 064311. URL <https://link.aps.org/doi/10.1103/PhysRevC.105.064311>.
- [50] Z. H. Sun, A. Ekström, C. Forssén, G. Hagen, G. R. Jansen, T. Papenbrock, [doi:10.1103/PhysRevX.15.011028](https://doi.org/10.1103/PhysRevX.15.011028), [Phys. Rev. X](https://link.aps.org/doi/10.1103/PhysRevX.15.011028) **15** (2025) 011028. URL <https://link.aps.org/doi/10.1103/PhysRevX.15.011028>.
- [51] Z. H. Sun, T. R. Djärv, G. Hagen, G. R. Jansen, T. Papenbrock, [doi:10.1103/PhysRevC.111.044304](https://doi.org/10.1103/PhysRevC.111.044304), [Phys. Rev. C](https://link.aps.org/doi/10.1103/PhysRevC.111.044304) **111** (2025) 044304. URL <https://link.aps.org/doi/10.1103/PhysRevC.111.044304>.
- [52] J. M. Yao, B. Bally, J. Engel, R. Wirth, T. R. Rodríguez, H. Hergert, [doi:10.1103/PhysRevLett.124.232501](https://doi.org/10.1103/PhysRevLett.124.232501), [Phys. Rev. Lett.](https://link.aps.org/doi/10.1103/PhysRevLett.124.232501) **124** (2020) 232501. URL <https://link.aps.org/doi/10.1103/PhysRevLett.124.232501>.
- [53] H. Hergert, S. Binder, A. Calci, J. Langhammer, R. Roth, [doi:10.1103/PhysRevLett.110.242501](https://doi.org/10.1103/PhysRevLett.110.242501), [Phys. Rev. Lett.](https://link.aps.org/doi/10.1103/PhysRevLett.110.242501) **110** (2013) 242501. URL <https://link.aps.org/doi/10.1103/PhysRevLett.110.242501>.
- [54] H. Hergert, [doi:10.3389/fphy.2020.00379](https://doi.org/10.3389/fphy.2020.00379), [A guided tour of ab initio nuclear many-body theory](https://www.frontiersin.org/journals/physics/articles/10.3389/fphy.2020.00379), *Frontiers in Physics* Volume 8 - 2020 (2020). URL <https://www.frontiersin.org/journals/physics/articles/10.3389/fphy.2020.00379>.
- [55] K. Tsukiyama, S. K. Bogner, A. Schwenk, [doi:10.1103/PhysRevC.85.061304](https://doi.org/10.1103/PhysRevC.85.061304), [Phys. Rev. C](https://link.aps.org/doi/10.1103/PhysRevC.85.061304) **85** (2012) 061304. URL <https://link.aps.org/doi/10.1103/PhysRevC.85.061304>.
- [56] K. Tsukiyama, S. K. Bogner, A. Schwenk, [doi:10.1103/PhysRevLett.106.222502](https://doi.org/10.1103/PhysRevLett.106.222502), [Phys. Rev. Lett.](https://link.aps.org/doi/10.1103/PhysRevLett.106.222502) **106** (2011) 222502. URL <https://link.aps.org/doi/10.1103/PhysRevLett.106.222502>.
- [57] T. D. Morris, J. Simonis, S. R. Stroberg, C. Stumpf, G. Hagen, J. D. Holt, G. R. Jansen, T. Papenbrock, R. Roth, A. Schwenk, [doi:10.1103/PhysRevLett.120.152503](https://doi.org/10.1103/PhysRevLett.120.152503), [Phys. Rev. Lett.](https://link.aps.org/doi/10.1103/PhysRevLett.120.152503) **120** (2018) 152503. URL <https://link.aps.org/doi/10.1103/PhysRevLett.120.152503>.
- [58] M. Anguiano, J. Egidio, L. Robledo, [doi:https://doi.org/10.1016/S0370-2693\(02\)02557-1](https://doi.org/10.1016/S0370-2693(02)02557-1), [Physica Letters B](https://www.sciencedirect.com/science/article/pii/S0370269302025571) **545** (1) (2002) 62–72. URL <https://www.sciencedirect.com/science/article/pii/S0370269302025571>.
- [59] M. V. Stoitsov, J. Dobaczewski, R. Kirchner, W. Nazarewicz, J. Terasaki, [doi:10.1103/PhysRevC.76.014308](https://doi.org/10.1103/PhysRevC.76.014308), [Phys. Rev. C](https://link.aps.org/doi/10.1103/PhysRevC.76.014308) **76** (2007) 014308. URL <https://link.aps.org/doi/10.1103/PhysRevC.76.014308>.
- [60] T. R. Rodríguez, J. L. Egidio, L. M. Robledo, [doi:10.1103/PhysRevC.72.064303](https://doi.org/10.1103/PhysRevC.72.064303), [Phys. Rev. C](https://link.aps.org/doi/10.1103/PhysRevC.72.064303) **72** (2005) 064303. URL <https://link.aps.org/doi/10.1103/PhysRevC.72.064303>.
- [61] P. Ring, P. Schuck, *The Nuclear Many-Body Problem*, Springer-Verlag, Berlin, Heidelberg, 1980.
- [62] K. Hebeler, S. K. Bogner, R. J. Furnstahl, A. Nogga, A. Schwenk, [doi:10.1103/PhysRevC.83.031301](https://doi.org/10.1103/PhysRevC.83.031301), [Phys. Rev. C](https://link.aps.org/doi/10.1103/PhysRevC.83.031301) **83** (2011) 031301. URL <https://link.aps.org/doi/10.1103/PhysRevC.83.031301>.

- [63] J. Simonis, K. Hebeler, J. D. Holt, J. Menéndez, A. Schwenk, Exploring sd -shell nuclei from two- and three-nucleon interactions, *Phys. Rev. C* 93 (2016) 011302. doi:[10.1103/PhysRevC.93.011302](https://doi.org/10.1103/PhysRevC.93.011302). URL <https://link.aps.org/doi/10.1103/PhysRevC.93.011302>.
- [64] J. Simonis, S. R. Stroberg, K. Hebeler, J. D. Holt, A. Schwenk, Saturation with chiral interactions and consequences for finite nuclei, *Phys. Rev. C* 96 (2017) 014303. doi:[10.1103/PhysRevC.96.014303](https://doi.org/10.1103/PhysRevC.96.014303). URL <https://link.aps.org/doi/10.1103/PhysRevC.96.014303>.
- [65] S. R. Stroberg, J. D. Holt, A. Schwenk, J. Simonis, Ab initio limits of atomic nuclei, *Phys. Rev. Lett.* 126 (2021) 022501. doi:[10.1103/PhysRevLett.126.022501](https://doi.org/10.1103/PhysRevLett.126.022501). URL <https://link.aps.org/doi/10.1103/PhysRevLett.126.022501>.
- [66] T. Miyagi, S. R. Stroberg, P. Navrátil, K. Hebeler, J. D. Holt, Converged ab initio calculations of heavy nuclei, *Phys. Rev. C* 105 (2022) 014302. doi:[10.1103/PhysRevC.105.014302](https://doi.org/10.1103/PhysRevC.105.014302). URL <https://link.aps.org/doi/10.1103/PhysRevC.105.014302>.
- [67] D. H. Glöckner, R. D. Lawson, Spurious center-of-mass motion, *Physics Letters B* 53 (4) (1974) 313–318. doi:[https://doi.org/10.1016/0370-2693\(74\)90390-6](https://doi.org/10.1016/0370-2693(74)90390-6). URL <https://www.sciencedirect.com/science/article/pii/0370269374903906>.
- [68] M. Wang, W. Huang, F. Kondev, G. Audi, S. Naimi, The ame 2020 atomic mass evaluation (ii). tables, graphs and references, *Chinese Physics C* 45 (3) (2021) 030003. doi:[10.1088/1674-1137/abddaf](https://doi.org/10.1088/1674-1137/abddaf). URL <https://dx.doi.org/10.1088/1674-1137/abddaf>.
- [69] National nuclear data center, <https://www.nndc.bnl.gov>.
- [70] B. Pritychenko, M. Birch, B. Singh, M. Horoi, Tables of $e2$ transition probabilities from the first $2+$ states in even-even nuclei, *Atomic Data and Nuclear Data Tables* 107 (2016) 1–139. doi:<https://doi.org/10.1016/j.adt.2015.10.001>. URL <https://www.sciencedirect.com/science/article/pii/S0092640X15000496>.
- [71] J. Henderson, G. Hackman, P. Ruotsalainen, S. Stroberg, K. Launey, J. Holt, F. Ali, N. Bernier, M. Bentley, M. Bowry, R. Caballero-Folch, L. Evitts, R. Frederick, A. Garnsworthy, P. Garrett, B. Jigmeddorj, A. Kilic, J. Lassen, J. Measures, D. Muecher, B. Olaizola, E. O’Sullivan, O. Paetkau, J. Park, J. Smallcombe, C. Svensson, R. Wadsworth, C. Wu, Testing microscopically derived descriptions of nuclear collectivity: Coulomb excitation of ^{22}Mg , *Physics Letters B* 782 (2018) 468–473. doi:<https://doi.org/10.1016/j.physletb.2018.05.064>. URL <https://www.sciencedirect.com/science/article/pii/S0370269318304283>.
- [72] S. R. Stroberg, J. Henderson, G. Hackman, P. Ruotsalainen, G. Hagen, J. D. Holt, Systematics of sd -shell nuclei with the valence-space in sd -shell, *Phys. Rev. C* 105 (2022) 034333. doi:[10.1103/PhysRevC.105.034333](https://doi.org/10.1103/PhysRevC.105.034333). URL <https://link.aps.org/doi/10.1103/PhysRevC.105.034333>.
- [73] J. M. Yao, J. Meng, P. Ring, D. Vretenar, Configuration mixing of angular-momentum-projected triaxial relationships, *Phys. Rev. C* 81 (2010) 044311. doi:[10.1103/PhysRevC.81.044311](https://doi.org/10.1103/PhysRevC.81.044311). URL <https://link.aps.org/doi/10.1103/PhysRevC.81.044311>.
- [74] T. R. Rodríguez, J. L. Egidio, Triaxial angular momentum projection and configuration mixing calculations, *Phys. Rev. C* 81 (2010) 064323. doi:[10.1103/PhysRevC.81.064323](https://doi.org/10.1103/PhysRevC.81.064323). URL <https://link.aps.org/doi/10.1103/PhysRevC.81.064323>.
- [75] A. O. Macchiavelli, H. L. Crawford, C. M. Campbell, R. M. Clark, M. Cromaz, P. Fallon, M. D. Jones, I. Y. Lee, M. Salathe, B. A. Brown, A. Poves, The $^{30}\text{Mg}(t, p)^{32}\text{Mg}$ “puzzle” reexamined, *Phys. Rev. C* 94 (2016) 051303. doi:[10.1103/PhysRevC.94.051303](https://doi.org/10.1103/PhysRevC.94.051303). URL <https://link.aps.org/doi/10.1103/PhysRevC.94.051303>.
- [76] N. Fukunishi, T. Otsuka, T. Sebe, Vanishing of the shell gap in $n = 20$ neutron-rich nuclei, *Physics Letters B* 296 (3) (1992) 279–284. doi:[https://doi.org/10.1016/0370-2693\(92\)91320-9](https://doi.org/10.1016/0370-2693(92)91320-9). URL <https://www.sciencedirect.com/science/article/pii/0370269392913209>.
- [77] T. Miyagi, Nuhamil: A numerical code to generate nuclear two- and three-body forces, *The European Physical Journal A* 59 (7) (2023) 150. doi:[10.1140/epja/s10050-023-01039-y](https://doi.org/10.1140/epja/s10050-023-01039-y). URL <https://doi.org/10.1140/epja/s10050-023-01039-y>.
- [78] S. R. Stroberg, <https://github.com/ragnarstroberg/imsrg>.
- [79] B. Bally, A. Sánchez-Fernández, T. R. Rodríguez, Symmetry-projected variational calculations with the numerical suite, *The European Physical Journal A* 57 (2) (2021) 69. doi:[10.1140/epja/s10050-021-00369-z](https://doi.org/10.1140/epja/s10050-021-00369-z). URL <https://doi.org/10.1140/epja/s10050-021-00369-z>.
- [80] B. Bally, T. R. Rodríguez, Symmetry-projected variational calculations with the numerical suite, *The European Physical Journal A* 60 (3) (2024) 62. doi:[10.1140/epja/s10050-024-01271-0](https://doi.org/10.1140/epja/s10050-024-01271-0). URL <https://doi.org/10.1140/epja/s10050-024-01271-0>.